PLASTOMETRIC STUDY OF HOT DEFORMATION BEHAVIOUR OF STEEL X10CRWMOVNB9-2

Ivo SCHINDLER [a], Radek MENDROK [a], Petr KAWULOK [a], Petr UNUCKA [b], Rostislav KAWULOK [a], Petr OPĚLA [a], Stanislav RUSZ [a], Rostislav TUROŇ [c], Petra TUROŇOVÁ [c], Aleš BUŘUTA [b]

[a] *VSB - Technical University of Ostrava, Faculty of Metallurgy and Materials Engineering, Ostrava, Czech Republic, EU, ivo.schindler@vsb.cz, radek.mendrok.st@vsb.cz*
[b] *Material and Metallurgical Research s.r.o., Ostrava, Czech Republic, EU, petr.unucka@mmvyzkum.cz*
[c] *Třinecké železárny a.s., Třinec, Czech Republic, EU, rostislav.turon@trz.cz*

Abstract

Phase composition of the studied high-alloy martensitic steel has been analyzed by metallographic methods, plastometric tests and thermodynamic calculations performed in the Thermo-Calc Software. Basic parameters of the formability and deformation resistance were determined depending on the forming temperature (800 - 1250 °C) and strain rate (0.1 - 17 s^{-1}). Continuous tests to fracture were performed at two individual plastometers which enable performance of the uniaxial tension (Gleeble 3800) and/or torsion (SETARAM). The results were processed into the illustrative 3D-maps that also reflect the effect of the phase composition at various deformation conditions. The mean forming temperature increased by tens of °C during some torsion tests due to deformation heating and this value had to be corrected. Since both plastometers work with different forming conditions and diverse state of stresses in the deformed sample, the mutual comparison of thus obtained results is interesting from the methodology viewpoint. The results of tension and torsion tests are quite compatible and display the positive influence of higher temperature and strain rate on the formability of the given steel.

Keywords: martensitic steel, torsion test, uniaxial tension test, hot formability, deformation resistance

1. INTRODUCTION

New ultra super critical boilers require materials with advanced creep properties to reach severe steam parameters with higher temperatures and higher pressures. The tube design temperature is limited to around 610 °C inside the combustion chamber. Critical components such as waterwall panels, reheaters, superheaters and main steam piping are easily manufactured from the new steels grades. Creep strength enhanced ferritic-martensitic steels such as T/P91 (X10CrMoVNb9-1) were developed to withstand the extreme operating conditions of new power plants and subsequently T/P92 (X10CrWMoVNb9-2) was developed to achieve good workability and comparable or better mechanical properties. More recent developments to produce new grades such as T/P911 (X11CrMoWVNb9-1-1) and T/P92 have improved mechanical properties at high temperatures, in particular an increase in creep strength of 10-20 % for 100,000 hours at 600 °C. This makes it possible to reduce the wall thickness of the pipes and consequently improve their resistance to thermal fatigue [1, 2].

T/P92 contains a W addition and a reduction in Mo content, compared to T/P91. This V-Nb-B microalloyed steel benefits from precipitation strengthening due to MX-type and $M_{23}C_6$-type precipitation which occurs during the tempering cycle. Solid-solution strengthening comes from W and Mo, while W-rich Laves phase precipitation is associated with increased resistance to creep. An addition of up to 0.006 % B also improves creep resistance. For grades T/P91, T/P911 and T/P92, the structure is purely tempered martensite, free of delta ferrite. The martensite is then tempered to promote carbide precipitation which results in an ideal strength and toughness combination. $M_{23}C_6$ is a major carbide in T/P92, followed by NbC. $M_{23}C_6$ tends to resist

coarsening for several thousands of hours. The Laves phase is found to finish its growth stage within 10,000 hours [3].

There exist a lot of studies concerning the welding and creep behaviour of various 9-12 % Cr steels (see [4-11] for example). Nevertheless, results related to the hot deformation behaviour of these materials are still missing. The aim of the performed plastometric experiments was to investigate the basic plasticity parameters of grade T/P92 (X10CrWMoVNb9-2) at temperatures relating to the seamless tubes rolling.

2. EXPERIMENTAL PROCEDURES

Chemical composition of the tested steel is presented in **Table 1**.

Table 1 Chemical composition in wt.%

C	Mn	Si	Cr	W	Mo	V	Nb	B	N
0.11	0.51	0.27	8.99	1.69	0.43	0.21	0.06	0.0034	0.0584

Most of the experimental material was taken from the hot-worked seamless tube, some samples were cut from the continuously cast billet for comparison. The samples with wrought structure were hot tested by torsion (plastometer SETARAM - MMV) and/or by uniaxial tension up to rupture (plastometer Gleeble 3800 - VŠB-TUO). Torsion test were performed after the uniform preheating at 1200 °C. The samples were cylindrical with diameter of 6 mm and length of the measured part 50 or 10 mm. The forming temperature varied from 900 to 1200 °C and the nominal strain rate from 0.1 to 2 s^{-1}. Peak stress and strain to fracture values were obtained from the flow stress curves.

Tension tests were realized after preheating at 1250 °C in the wider range of experimental conditions: forming temperature from 800 to 1250 °C, mean strain rate from 0.16 to 17 s^{-1} (depending on the stroke rate 1.9 - 190 $mm \cdot s^{-1}$ and on the total elongation). The measured (i.e. homogeneously heated) zone of the sample had dimensions as follows: diameter 10 mm, length 20 mm. Ultimate hot tensile strength as well as relative total elongation of the sample were determined.

2.1 Deformation resistance

The 3D-maps in **Fig. 1** represent the deformation resistance values obtained experimentally and processed by the Surfer 8 Software.

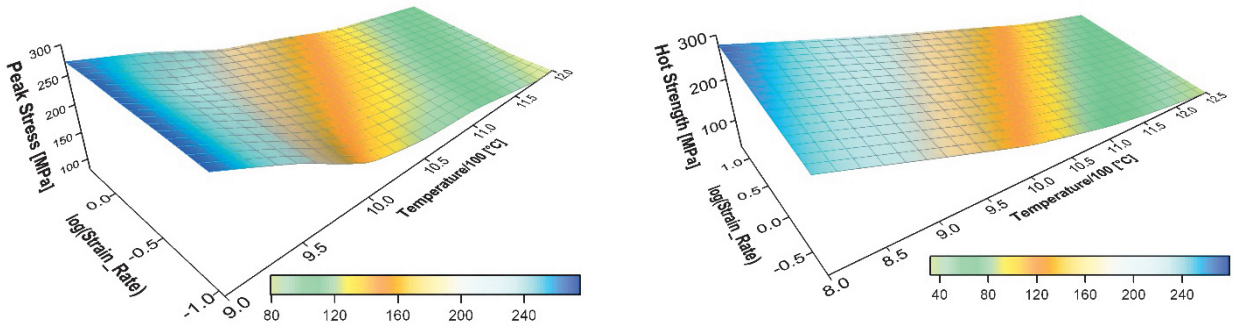

a) results of torsion b) results of tension

Fig. 1 Deformation resistance as a function of temperature and strain rate

The results of torsion and tension tests are quite comparable though the strength at tension is a conventional quantity only, whereas the peak (i.e. maximum) stress at torsion represents a true flow stress. It is evident that the deformation resistance of the studied material is influenced particularly by temperature and less by strain

rate. The obtained trends are overall monotonous, with a slight edge near by 1050 °C. Metallography did not disclose any marked differences in the phase composition at various temperatures - the microstructure after heating and quenching was always formed by martensite, only at temperature 1200 °C the small amount of delta-ferrite at grain boundaries was detected - see **Fig. 2**.

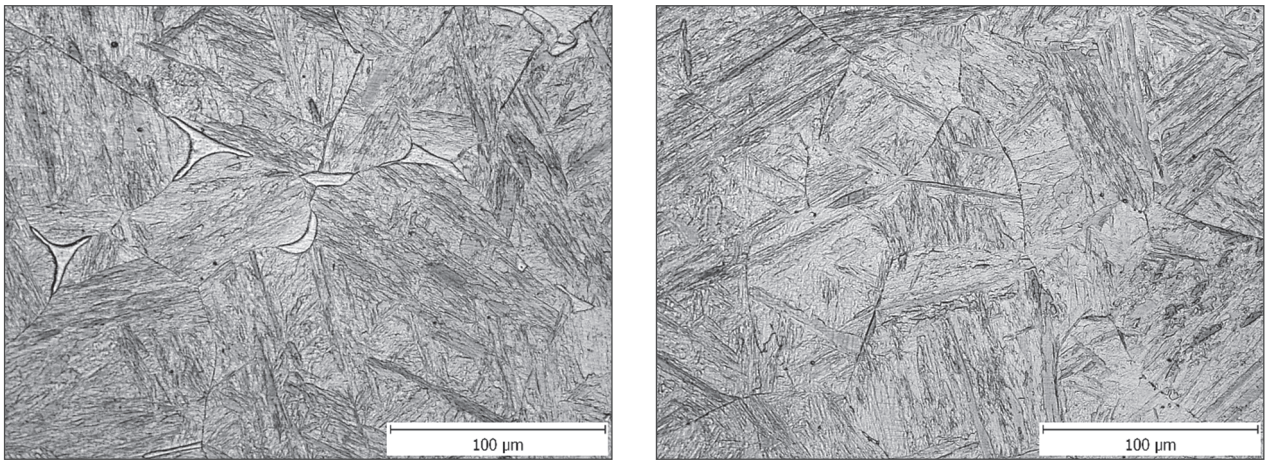

a) 1200 °C b) 1030 °C

Fig. 2 Quenched microstructure after heating at selected temperatures

The phase composition of the studied martensitic steel has been analyzed by thermodynamic calculations performed in the Thermo-Calc Software as well. **Table 2** shows that the ferrite can be expected at the temperatures above 1178 °C, or below 895 °C (which was not confirmed by metallography). Change of deformation behaviour close by 1050 °C could be caused by the VN precipitation.

Table 2 Equilibrium phase composition calculated by the Thermo-Calc Software

from T [°C]	Phase	to T [°C]
>1504	Liquid	
1504	Liquid + BCC	1499
1499	Liquid + BCC + FCC + TiN	1427
1427	BCC + FCC + TiN	1215
1215	BCC + FCC + TiN + Nb(C,N)	1178
1178	FCC + TiN + Nb(C,N)	1058
1058	FCC + TiN + Nb(C,N) + VN	895
895	BCC + FCC + TiN + Nb(C,N) + VN + $M_{23}C_6$	824
<824	BCC + TiN + Nb(C,N) + VN + $M_{23}C_6$	

2.2 Formability

The obtained experimental data related to the hot formability of the studied steel seem to be rather controversial - see **Fig. 3**.

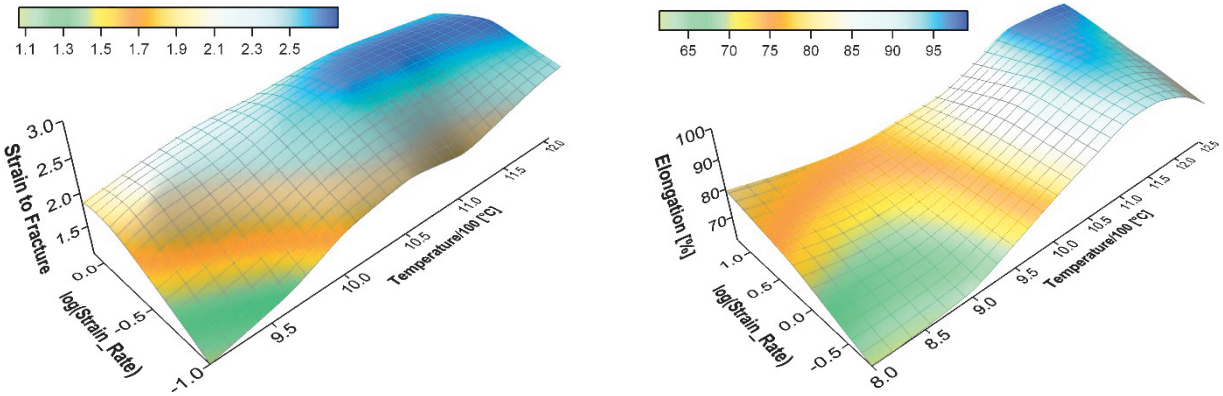

a) results of torsion b) results of tension

Fig. 3 Formability as a function of temperature and strain rate

Influence of strain rate is ambiguous and the effect of temperature is marked only at the values below 1000 °C in the case of the torsion tests. The problems were caused by the relatively narrow range of the experimental conditions as well as by the relatively massive deformation heating at high strains. The sample's temperature increased by tens of °C at torsion (especially at low temperatures and higher strain rates) and thus the real forming temperature differed from the nominal value. The 3D-map had to be based on the mean temperatures values calculated for every torsion test.

Tensile tests showed the more reliable results with a much lesser scatter of the hot formability data. The best plastic properties were observed at the highest strain rates (up to 17 s^{-1}) and temperature of about 1150 °C. Combination of low temperature (below 950 °C) and low strain rate (0.16 s^{-1}) yielded in a drop of formability. Also the highest forming temperatures (over 1200 °C) deteriorate the plastic properties very intensively due to the material's overheating or even burning - it is interesting that such effect is more pronounced at low strain rates.

Plastic properties of the as-cast steel were studied by tension tests for comparison (only at temperature of 1150 °C and strain rate of 1.6 s^{-1}). Samples machined from the dendritic zone (crosswise the huge columnar grains) exhibited the elongation lower by about 8 % only in comparison with the wrought material. Surprisingly the worst formability was observed in the zone of great equiaxed grains just below the columnar crystals, towards the central part of the continuously cast product - with a drop of elongation by about 24 % according to the material taken from the rolled tube.

2.3 Plastometric study of phase transformations

The complementary plastometric study was performed at Gleeble 3800 as a simplified dilatometric test. The cylindrical sample with diameter of 8 mm and height of 12 mm was subjected to the resistance heating between two fixed jaws. The constant heating rate was 5 °C·s^{-1} and the cooling rate was 1 °C·s^{-1}, respectively. The changes of the sample's volume yielded in the force acting on the jaws that was recorded as a function of temperature - (see **Fig. 4**).

The marked phase transformation were detected close by 850 °C (probably due to $M_{23}C_6$ dissolving/precipitation - see **Table 2**), at about 1070 °C (particles of VN) and over about 1130 °C at heating (which can not be simply explained to date). As the metallographic analyses did not prove the existence of ferrite at low temperatures (in contradiction with **Table 2**), the observed drop of formability at temperatures below 950 °C can be explained by the $M_{23}C_6$ particles only.

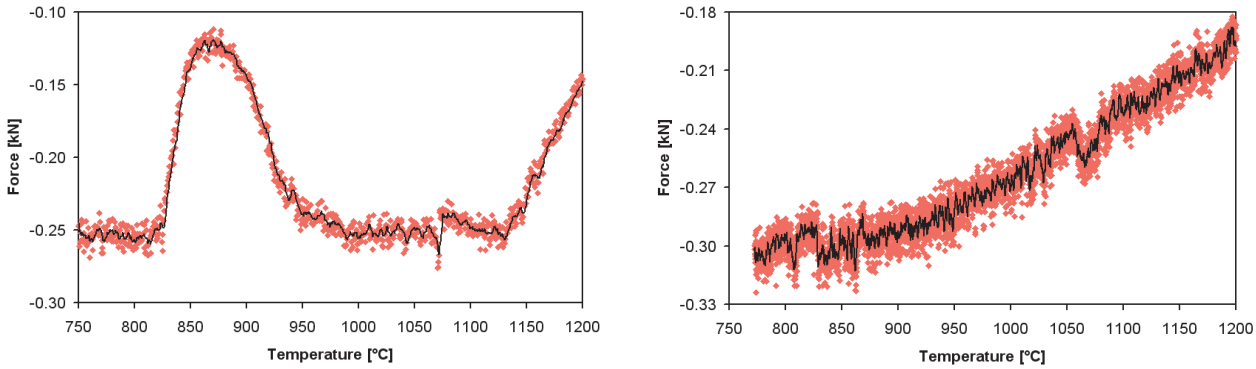

a) heating by 5 °C·s^{-1} b) cooling by 1 °C·s^{-1}

Fig. 4 Results of the simplified dilatometric tests (points - measured values; lines - averaged trends)

CONCLUSIONS

Phase composition of the studied martensitic steel X10CrWMoVNb9-2 was analyzed by metallographic methods, plastometric tests and thermodynamic calculations performed in the Thermo-Calc Software and some discrepancies between calculations and experiments were demonstrated. Basic parameters of the formability and deformation resistance were determined depending on the forming temperature (800 - 1250 °C) and strain rate (0.1 - 17 s^{-1}). Continuous tests to fracture were performed at two individual plastometers which enable performance of the uniaxial tension and/or torsion. The results were processed into the illustrative 3D-maps that also reflect the effect of the phase composition ($M_{23}C_6$ particles) at various deformation conditions. The advantage of the torsion plastometer presented at study of deformation resistance is that the twisted sample keeps its dimensions and calculation of the real flow stress is possible. The obtained data of the strength properties can be used for fast prediction of the power-force parameters of the operational forming technologies. On the other hand, the uniaxial tension test gave much better results concerning the formability. The mean forming temperature increased by tens of degrees of Celsius during some torsion tests due to deformation heating. The results of plastometric tests displayed the positive influence of higher temperature and strain rate on formability of the given steel. Influence of the initial structure (wrought vs as-cast state) on the hot formability of the studied steel was quantified.

ACKNOWLEDGEMENTS

The research was supported by the projects FR-TI3/374 (financed by MPO ČR), LO1203 (MŠMT ČR) and SP2014/100 (MŠMT ČR).

REFERENCES

[1] VAILLANT, J. C., et al. *International Journal of Pressure Vessels and Piping*. 2008, Vol. 85, pp. 38-46.

[2] PCC ENERGYGROUP P92 X10CrWMoVNb9-2 [online]. [viewed 2014-2-26]. Available from: http://pccenergygroup.com/assets/klad_docs/120409_WG_P92_Brochure.pdf

[3] SRINIVAS PRASAD, B. S., et al. Computer Coupling of Phase Diagrams and Thermochemistry. *CALPHAD: Computer Coupling of Phase Diagrams and Thermochemistry*. 2012, Vol. 36, pp. 1-7.

[4] ŁOMOZIK, M., ZEMAN, M., BRÓZDA, J. Modern martensitic steels for power industry. *Archives of Civil and Mechanical Engineering*. 2012, No. 12, pp. 49-59.

[5] BUMJOON, K., CHANSEO, J., BYEONGSOO, L. Creep behavior and microstructural damage of martensitic P92 steel weldment. *Materials Science and Engineering A*. 2008, Vol. 483-484, pp. 544-546.

[6] FOURNIER, B., et al. Comparison of various 9-12%Cr steels under fatigue and creep-fatigue loadings at high temperature. *Materials Science and Engineering A*. 2011, Vol. 528, No. 22-23, pp. 6934-6945.

[7] XUE, W., et al. Creep rupture behaviour of P92 steel weldment. *Engineering Failure Analysis*. 2011, Vol. 18, No. 1, pp. 186-191.

[8] HU, P., et al. Microstructure Evolution of a 10Cr Heat-Resistant Steel during High Temperature Creep. *Journal of Materials Science & Technology*. 2011, Vol. 27, No. 4, pp. 344-351.

[9] ZIELIŃSKA-LIPIEC, A., et al. Evolution of dislocation density, size of subgrains and MX-type precipitates in a P91 steel during creep and during thermal ageing at 600 °C for more than 100,000 h. *Materials Science and Engineering A*. 2010, Vol. 527, No. 16-17, pp. 4062-4069.

[10] BESSON, J., et al. Analysis of creep lifetime of a ASME Grade 91 welded pipe. *Engineering Fracture Mechanics*. 2009, Vol. 76, No. 10, pp. 1460-1473.

[11] XUE, W., et al. Microstructure and type IV cracking behavior of HAZ in P92 steel weldment. *Materials Science and Engineering: A*. 2012, Vol. 552, pp. 493-501.